

Relating Plastic Properties to Microstructure by Linking FE Simulations with Microstructure Analysis

Hasso Weiland, Michael E Karabin and Thomas N Rouns

Alcoa Technical Center, 100 Technical Drive, Alcoa Center, PA 15068, U.S.A.

Microstructure analysis using various imaging techniques has become a routine tool in the aluminum industry for quantifying the processing-property relationship for manufactured products. To improve the correlation between microstructure analysis and mechanical properties, imaging filters were calculated from simulations of the mechanical process in consideration. Specifically it will be shown how the stress intensity field at a crack tip during cyclic loading, calculated from FE simulations, is used as a weighted filter to determine the number of particles for a given microstructure contributing to a fatigue process.

Sister ingots made of the same alloy received the same thermal and hot rolling history but were cold rolled to the same gauges using different cold rolling schedules. Quantitative microstructure analysis showed that second phase volume fraction and size distributions are the same for both products. However, during mechanical testing fatigue crack growth values showed significant differences for samples produced by the two processing paths. Using FE simulations of plastic zone sizes and shapes calculated from the respective mechanical properties, gradient filters for image analysis were generated. This highlighted discerning differences in microstructures from samples which have similar first order characteristics.

Keywords: Microstructure characterization, image analysis, fatigue, aluminum alloys, FE simulation, plastic zone size, microstructure property relation .

1. Introduction

The performance of aluminum alloys is strongly related to its microstructure. In general, the combination of solute, precipitates and second phase particles, grain size and crystallographic texture determines the mechanical properties of a given aluminum alloy. Consequently, if composition and thermo-mechanical history for a metal sample is similar, then one should anticipate that mechanical properties are similar as well.

However, in a processing trial it was found that this is not always the case. Sister ingots, from the same alloy that were cast simultaneously and homogenized together, followed by the same hot rolling schedule. The metal was finished on two different cold rolling mills to the same sheet gauge. One coil was finished on a tandem mill, labeled as Processing Path A, while the second coil was finished on a reversing mill, labeled in the following as Processing Path B. As a consequence of the ingots being cast from the same melt and being homogenized together, the volume fraction and size distribution of constituent particles, which are second phase

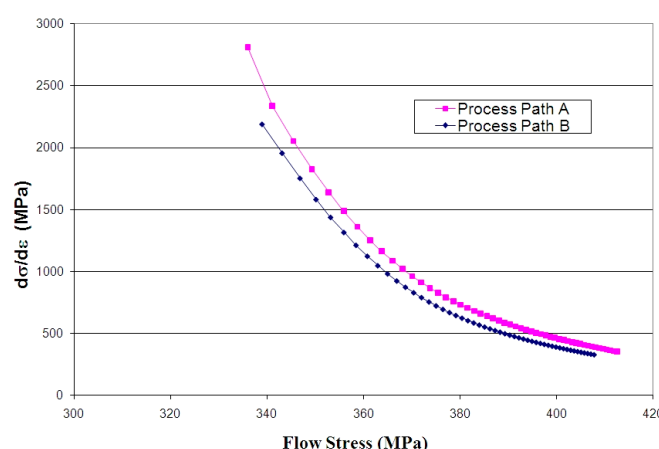


Fig. 1 Hardening Curves for both Processing Paths

particles formed during solidification and then refined during rolling, was the same as determined by quantitative metallurgy (avg particle size: $3.2 \mu\text{m}^2$, avg volume fraction: 0.78%). Yet while all microstructural parameters indicated no difference between both products, significant differences in fatigue crack growth rates (da/dN) of the final sheet resulted. At a Δk of $25 \text{ MPa}\sqrt{\text{m}}$, the values were $2.3 \cdot 10^{-3} \text{ mm/cycle}$ and $1.8 \cdot 10^{-3} \text{ mm/cycle}$, respectively. A detailed analysis showed that the stress strain curves of both materials varied slightly in the strain hardening rate (Fig. 1) as well as that minor differences in crystallographic texture were present (not shown here). It was thus concluded that small differences in the yield surface cause differences in the plastic zone size. This would result in a different number of constituent particles in each plastic zone contributing to the crack growth rate during cyclic loading.

2. Linking plastic behavior with microstructure characterization

2.1 Simulation of plastic zone sizes

Using the measured hardening behavior, the change in plastic zone size at the crack tip between two load cycles during fatigue testing was determined by employing finite elements simulations. The results from the two processing paths use the same geometry at two different loadings: $\Delta k=25$ and $35 \text{ MPa}\sqrt{\text{m}}$. The loading consists of $1\frac{1}{2}$ cycles of a tensile load applied normal to the plane of crack growth (Mode I) in a center crack panel. Figure 2 is a contour plot of the difference in plastic strain between the two peak loads at $1\frac{1}{2}$ and $\frac{1}{2}$ cycles for $\Delta k=25 \text{ MPa}\sqrt{\text{m}}$ and for $\Delta k=35 \text{ MPa}\sqrt{\text{m}}$. The two processing paths produced slightly material behaviors as described above. The strain hardening curves are depicted in Figure 1 and the relationship is described in Ref [1]. The differences in texture for the two different flow paths are characterized by the input to the yield surface relationship which is described in Ref [2,3]. The length of each side in the FEM mesh corresponded to $40.6 \mu\text{m}$. This enabled scaling of each plastic zone shape to the scale of the images taken of the microstructure.

The incremental change in plastic zone size shows as expected the highest plastic strains near the crack tip, with gradually smaller strains towards the unaffected matrix. For a given Δk , the shapes of each calculated plastic zone change and the respective gradients from high to low plastic strain within each zone only differ slightly for both processing paths. Due to the similarity of the figures, especially as reproduced here, only one plastic zone size for each Δk is shown. However, it was assumed that these small differences contribute to the observed differences in crack growth rates in the following:

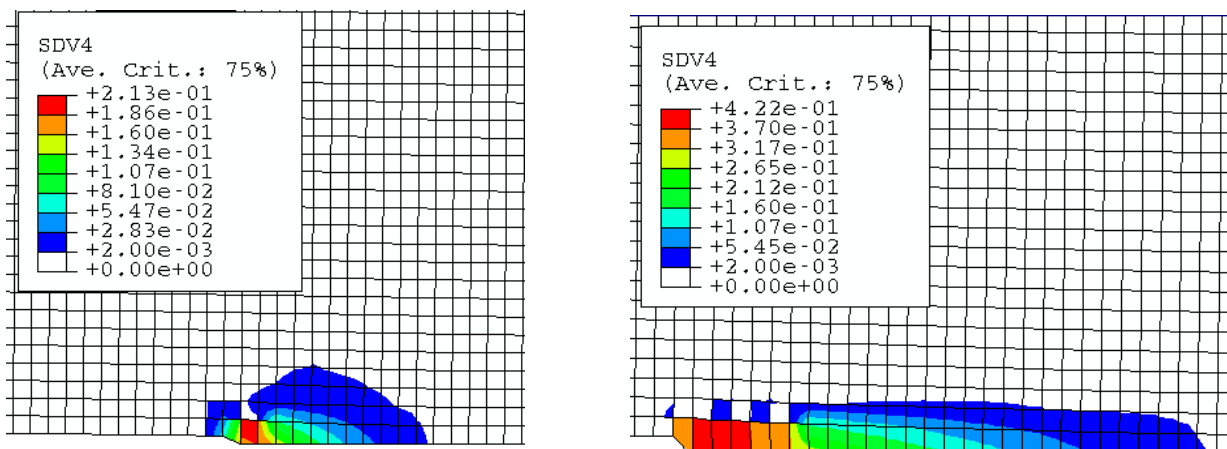


Fig 2: Incremental change in plastic zone size between two load cycles during fatigue testing from FE simulation at two different Δk : a) $25 \text{ MPa}\sqrt{\text{m}}$ b) $35 \text{ MPa}\sqrt{\text{m}}$
Color scale corresponds to different changes in plastic strain between load changes.

during each loading cycle, a slightly different volume of material, thus different number of particles is probed by the plastic strain field. Thus it was the objective to evaluate the microstructure based on the differences in plastic zone character.

2.2 Microstructure Characterization

From each sample, an area of 5 mm square was mapped by Backscattered Electron (BSE) imaging in a Scanning Electron Microscope (SEM, FEI Sirion) by stitching images taken at a magnification of 250x with a resolution of 0.5 $\mu\text{m}/\text{pixel}$. The resolution ensured that all second phase particles affecting the fatigue performance were captured. The sample surface was prepared at the sheet mid-thickness ($T/2$), containing the rolling and the transverse direction. Figure 3 shows a subset of one montage. This figure consists of 3 by 5 frames taken by SEM.

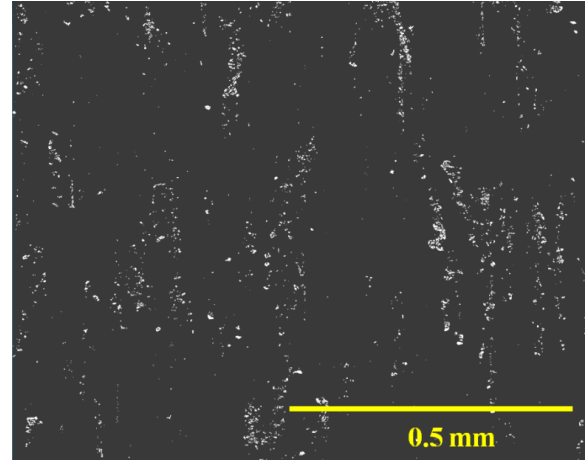


Fig 3: Constituent particles characterized by BSE-SEM in the rolling plane at mid-thickness of the sheet. A subset of 5x3 frames of the whole area analyzed is shown.

2.3 Filter Generation

A plastic zone filter was established based on each calculated plastic zone shape change, converting the decreasing strain in the plastic zone change (Fig. 4b) to a decreasing intensity in the filter (Fig. 4c). The highest strain at the crack tip corresponds to the highest level in color white. This weighted intensity filter was then applied to each map of second phase particles from both processing paths. The difference is clearly visible when comparing

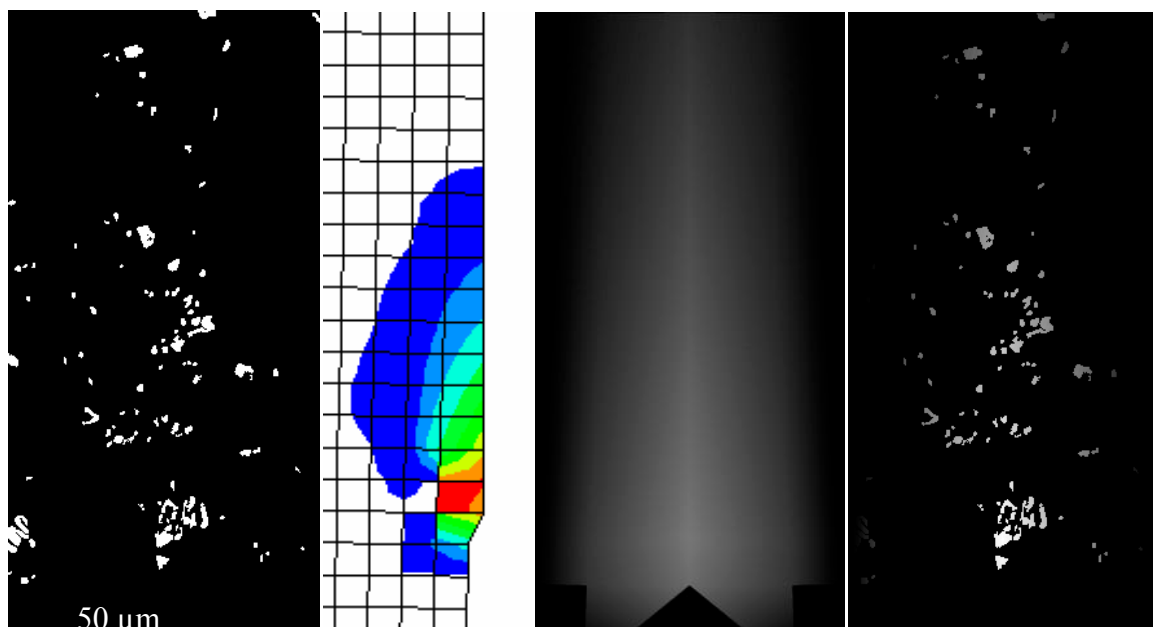


Fig 4: Applying FEM-based plastic zone shape to the images of second phase particles
 a) Cutaway from Fig 3 (note: difference in scale); b) half of simulated plastic zone size
 c) weighted intensity filter based on 4b); d) application of 4c to same area shown in 4a.

Fig 4a and d: in the unweighted image of the microstructure, all particles within the field of view would be counted equally. However, when applying the weighted filter from Fig 4c to Fig 4a, it becomes clear how particles in the vicinity of the crack tip contribute more to the fatigue process than particles further away.

2.4 Image Analysis and Data Representation

The weighted intensity filter was applied to each large area microstructure map by positioning the filter such that the crack tip, thus the highest strain intensity, coincides with a constituent particle in the map. For each placement of the filter in the microstructure the intensities of all pixels within the view of the filter were summed. Thus a constituent particle next to the crack tip was counted more than a particle near the edge of the plastic zone. The filter was then placed on the next constituent particle etc, until the whole area characterized by SEM was analyzed. The summed intensity for each filter placement was then plotted in Fig. 5, corresponding to a weighted particle area within a plastic zone. Each data point corresponds to one placement of the filter.

Fig. 5 shows the collected data for a microstructure analyzed using intensity weighted filters as described above. The horizontal spread in each data set is an applied jitter to better discern individual data points. The wide horizontal bars correspond to the 95% confidence index (CI) of the mean, the box frames the mean with the 25% and 75% CI. The plot shows that for a given Δk , the area fraction of particles can vary significantly within a plastic zone. It also is clear that for a larger Δk , much more particles are encompassed by the plastic zone.

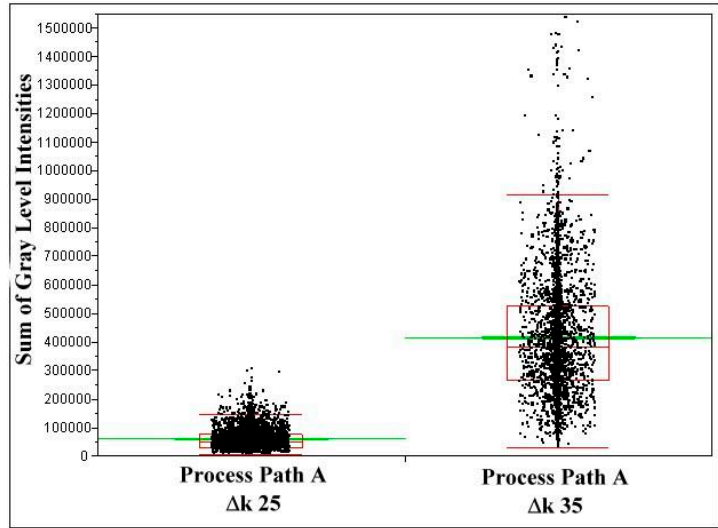


Fig. 5 Scatter plot of summed intensities for two different plastic zone sizes, based on the analysis of the microstructure created in processing path A

3. Results and Discussion

Comparing the data (Fig. 6) obtained as outlined above clearly shows differences between both materials: the mean weighted intensity levels for processing path A are always statistically lower than those determined for processing path B. This holds for both values of stress intensity factors, with the difference even more pronounced at the higher stress intensity of $\Delta k=35 \text{ MPa}\sqrt{\text{m}}$ (Fig 6b). This means that in average, the plastic zone of the material fabricated by processing path A contains a lower number of constituent particles than the material from processing path B. Each constituent particle actively participates in the crack growth by being sites for void nucleation and linking [4]. Consequently a lower number of constituent particles means a lower probability for void nucleation and linking, contributing to a slower crack growth rate. The difference between both materials becomes even more pronounced when comparing the area fraction of particles at different plastic strain levels ahead of the crack tip within the plastic zone simulated for a Δk of 25 $\text{MPa}\sqrt{\text{m}}$ (Fig. 7). While directly at the crack tip, differences in area fraction between both materials are insignificant. However, ahead of the crack tip, the constituent particle fraction for the material processed by Path A is always lower than the material from process path B. This is important as it is exactly in the area where intermediate strain levels are present that voids form, providing opportunity for the crack to grow by void linking.

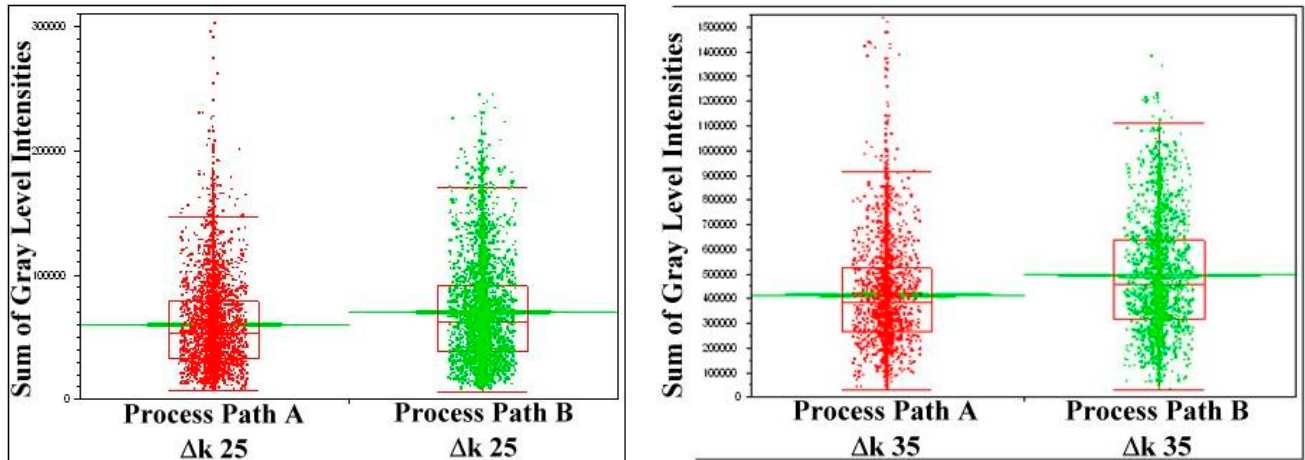


Fig. 6 Weighted particle area within plastic zones for two different processing path at two different Δk s a) $\Delta k = 25 \text{ MPa}/\text{m}$ b) for $\Delta k = 35 \text{ MPa}/\text{m}$

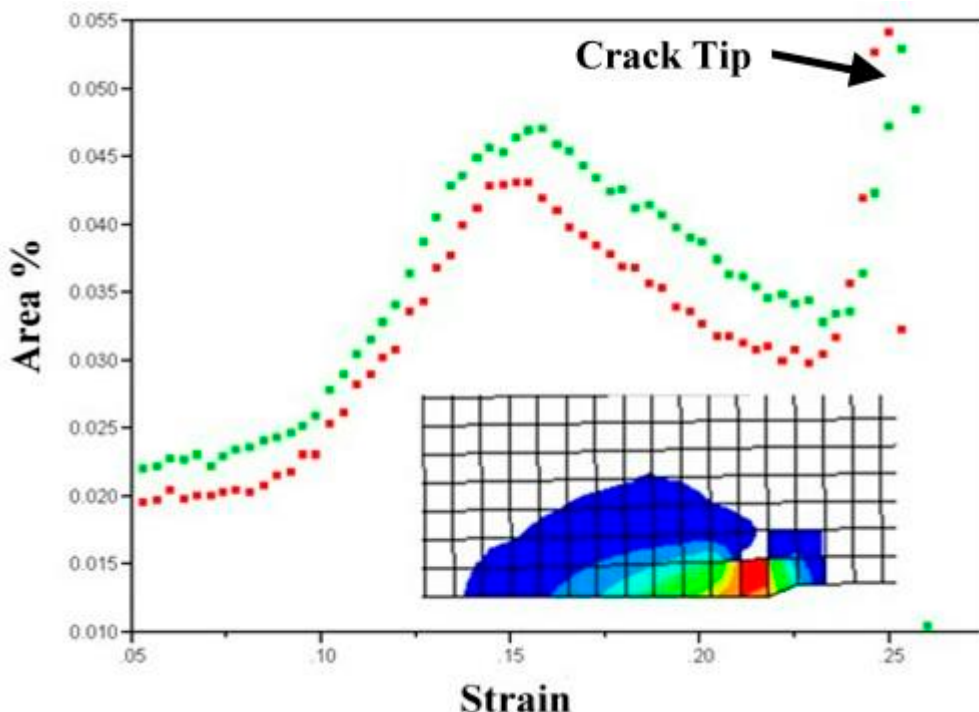


Fig. 7 Area fraction of constituent particles at different strain levels within the simulated plastic zone for a Δk of $25 \text{ MPa}/\text{m}$. Upper curve (green) are data for processing path A, lower curve (red) are data for processing path B. For illustration purpose, Fig 4 b is pasted into the graph in the orientation of the data on the X-axis.

By considering the respective yield surface and hardening rate for the microstructure analysis, it was possible to identify differences in two products with very similar thermo-mechanical history. It was shown that a slight difference in yield surface and hardening rate made a significant difference in the interaction of the plastic zone at a crack tip with the microstructure. The origin of the differences in yield surface and hardening rate are found in the effect both cold rolling operations have on the second order microstructure characteristics. Finishing a product on a tandem mill vs. on a reversing

mill causes differences in stored energy affecting the hardening rate. Additionally, achieving the same gauge during straight rolling vs. reverse rolling affects the through-thickness gradient in texture, thus affecting the yield surface of each product.

4 Summary

Two products fabricated with the same thermo-mechanical history showed the same first order microstructure characteristics, yet their crack growth rates during fatigue testing differed by 22%. By applying FE simulations, it was shown that slight differences in yield surface and hardening rate have an effect on the size and shape of the stress intensity field, the plastic zone, at the crack tip of both products. When the respective simulated plastic zones were used to construct gradient filters for microstructure analysis, it was shown that the number of constituent particles actively participating in each change during cycling loading differed sufficiently to cause the observed differences in crack growth rates.

In summary, relating plastic properties to microstructure by linking FE simulations with microstructure analysis allowed discerning differences in microstructures from samples which have similar first order characteristics.

References

- [1] F. Barlat, M. V. Glazov J. C. Brem and D. J. Lege. *Int. J. Plasticity* 18, pp 919-939 (2002)
- [2] F. Barlat, J.C. Brem, J.W. Yoon, K. Chung, R.E. Dick, D.J. Lege, F. Pourboghrat, S.-H. Choi, E. Chu, *Int. J. Plasticity*, Vol. 19, No.9, pp. 1297-1319 (2003)
- [3] J.W. Yoon, F. Barlat. R.E. Dick, *Int. J. Plasticity*, Vol. 20, No.9, pp. 495-522 (2004)
- [4] H. Weiland, J. Nardiello, S. Zaefferer[✉]S. Cheong[✉]J. Papazian and Dierk Raabe, *Engineering Fracture Mechanics* 76, pp. 709–714 (2009)